Random Decrement

Asmussen, J. C.; Ibrahim, R.; Brincker, Rune

Published in:
Proceedings of the 16th International Modal Analysis Conference, Santa Barbara, California, USA, Feb. 1998

Publication date:
1998

Document Version
Publisher's PDF, also known as Version of record

Random Decrement: Identification of Structures Subjected to Ambient Excitation

J.C. Asmussen[1], S.R. Ibrahim[2] & R. Brincker[1]
[1]Department of Building Technology and Structural Engineering
Aalborg University, Sohngaardsholmsvej 57, 9000 Aalborg, Denmark.
[2]Department of Mechanical Engineering, Old Dominion University,
238 Kaufman/Duckworth Hall, Norfolk, Virginia, USA.

Abstract *This paper demonstrates how to use the Random Decrement (RD) technique for identification of linear structures subjected to ambient excitation. The theory behind the technique will be presented and guidelines how to choose the different variables will be given. This is done by introducing a new concept: Quality Assessment. The identification process and quality assessment is illustrated by an analysis of the ambient response of a two-span concrete bridge.*

Nomenclature

a_1, a_2, b_1, b_2	Triggering levels.
$\mathbf{C}$	Damping Matrix.
D_{XX}, D_{YY}	Auto RD functions.
D_{XY}, D_{YX}	Cross RD functions.
$E[\cdot\|\cdot]$	Conditional mean value.
f	Natural frequency.
$\mathbf{K}$	Stiffnes matrix.
$\mathbf{M}$	Mass matrix.
N	Number of triggering points.
$\mathbf{q}_0$	Initial modal conditions.
t, τ	Time variables.
$T_{X(t)}$, $T_{Y(t)}$	Triggering conditions.
$T_{X(t)}^{G_A}$	Applied general triggering condition.
$T_{X(t)}^{E}$	Local extremum triggering condition.
$T_{X(t)}^{L}$	Level crossing triggering condition.
$T_{X(t)}^{P}$	Positive point triggering condition.
$T_{X(t)}^{Z}$	Zero crossing triggering condition.
$X(t)$, $Y(t)$	Stochastic processes.
$x(t)$, $y(t)$	Realization of $X(t)$, $Y(t)$.
R_{XX}, R_{YY}	Auto correlation functions.
R_{XY}, R_{YX}	Cross correlation functions.
$\mathcal{E}$	Error function.
$\mathbf{\Phi}$, $\tilde{\mathbf{\Phi}}$	Mode shape matrix.
$\mathbf{\Lambda}$, $\tilde{\mathbf{\Lambda}}$	Diagonal matrix with eigenvalues.
ζ	Damping ratio.
DOF	Degrees of Freedom.
FFT	Fast Fourier Transform.
ITD	Ibrahim Time Domain.
PTD	Polyreference Time Domain.
RD	Random Decrement.

1 Introduction

The RD technique was introduced by H.A. Cole during the late 1960s and early 1970s, see Cole [1], [2], [3] and [4] as an alternative to the FFT algorithm for the analysis of response measurements only. Cole mainly applied the technique to the measured vibrations of space structures subjected to unmeasurable ambient excitation. The RD technique is attractive since the implementation is simple and the estimation time is low. The principle is to estimate RD functions by averaging time segments of the mesurements, which have been selected under certain conditions. From the RD functions the modal parameters of the structure can be extracted using methods developed to extract modal parameters from free decays or correlation functions.

Since the development of this technique, the theory behind the technique has been extended and the technique has been applied to a large variety of structures. Nasir et al. [5] applied the RD technique to vibrations of offshore platforms, Siviter et al. [6] used the technique for measuring railway vehicle kinematics, Al-Sannad et al. [7] used the technique in soil testing and the technique has been applied in ambient testing of bridges, see e.g. Asmussen et al. [8], [9], [10] and Fasana et al. [11].

The purpose of this paper is to describe a procedure for the analysis of vibrations of ambient excited structures using the RD technique. The theory behind the technique is described and a recipe for the application of the technique is given.

The natural starting point is the definition and the estimation of RD functions which is shown in section 2 . Section 3 describes how RD functions can be interpreted as free decays of the structure, and section 4 describes how RD functions can be interpreted as correlation functions. These two interpretations support each other and constitute the theoretical background for the RD technique. Section 5 describes how the structures and the loads are modelled. Section 6 describes how the triggering conditions can be chosen using quality assessment. Section 7 describes how the modal parameters can be extracted from the RD functions. To illustrate the application of the above theoretical statements and guidelines a two-span concrete highway bridge is identified.

2 Definition and Estimation

To describe the RD technique two stationary stochastic processes, $X(t)$ and $Y(t)$ are considered. The ambient measurements are considered to be realizations of $X(t)$ and $Y(t)$. The auto, D_{XX}, D_{YY}, and cross, D_{YX}, D_{XY}, RD functions are defined as conditional mean values

$$D_{XX}(\tau) = E[X(t+\tau)|T_{X(t)}] \quad (1)$$

$$D_{YX}(\tau) = E[Y(t+\tau)|T_{X(t)}] \quad (2)$$

$$D_{YY}(\tau) = E[Y(t+\tau)|T_{Y(t)}] \quad (3)$$

$$D_{XY}(\tau) = E[X(t+\tau)|T_{Y(t)}] \quad (4)$$

The first index refers to the process where the mean value is calculated and the second index refers to the process where the condition is fulfilled. The conditions $T_{X(t)}$ and $T_{Y(t)}$ are denoted triggering conditions and an actual time, t, where the condition is fulfilled, is denoted a triggering point. If n measurements are available it is possible to estimate n different sets of RD functions each containing n functions. This corresponds to the number of correlation functions, which can be estimated from the n measurements. D_{XX}, D_{YX} in eqs. (1), (2) and D_{XY}, D_{YY} in eqs. (3), (4) constitute two different sets of RD functions, e.g.

$$\left[\begin{pmatrix} \text{Set 1} \\ D_{XX}(\tau) \\ D_{YX}(\tau) \end{pmatrix} \begin{pmatrix} \text{Set 2} \\ D_{XY}(\tau) \\ D_{YY})(\tau) \end{pmatrix} \right] \quad (5)$$

If the processes are assumed to be ergodic the RD functions can be estimated unbiased as

$$\hat{D}_{XX}(\tau) = \frac{1}{N}\sum_{i=1}^{N} x(t_i+\tau)|T_{x(t_i)} \quad (6)$$

$$\hat{D}_{YX}(\tau) = \frac{1}{N}\sum_{i=1}^{N} y(t_i+\tau)|T_{x(t_i)} \quad (7)$$

$$\hat{D}_{XY}(\tau) = \frac{1}{N}\sum_{i=1}^{N} x(t_i+\tau)|T_{y(t_i)} \quad (8)$$

$$\hat{D}_{YY}(\tau) = \frac{1}{N}\sum_{i=1}^{N} y(t_i+\tau)|T_{y(t_i)} \quad (9)$$

where $x(t)$ and $y(t)$ are the measurements and N is the number of triggering points. The estimation of RD functions is very simple. It only involves the detection of triggering points and averaging of data time segments.

The triggering condition simply describes a requirement for the initial condition of the time segments in the averaging process at the time lag $\tau = 0$. Several different triggering conditions have been used. They can all be considered as specific formulation of the applied general triggering condition, $T_{X(t)}^{G_A}$

$$T_{X(t)}^{G_A} = \{a_1 \leq X(t) < a_2,\ b_1 \leq \dot{X}(t) < b_2\} \quad (10)$$

The most frequently used triggering conditions are level crossing, $T_{X(t)}^{L}$, positive point, $T_{X(t)}^{P}$, local extremum, $T_{X(t)}^{E}$, and zero crossing, $T_{X(t)}^{Z}$

$$T_{X(t)}^{L} = \{X(t) = a\} \quad (11)$$

$$T_{X(t)}^{P} = \{a_1 \leq X(t) < a_2\} \quad (12)$$

$$T_{X(t)}^{E} = \{a_1 \leq X(t) < a_2, \dot{X}(t) = 0\} \quad (13)$$

$$T_{X(t)}^{Z} = \{X(t) = a, \dot{X}(t) > 0\} \quad (14)$$

$T_{X(t)}^{P}$ is the most versatile condition, since the number of triggering points can be adjusted by changing the triggering levels. The number of triggering points controls the estimation time and the accuracy of the estimates. Therefore, it is recommended to use the positive point triggering condition in application to ambient data unless the measurements are extremely long. If the triggering levels are chosen as $a_1 \approx a_2$ the positive point equals the level crossing triggering condition.

3 RD Functions and Free Decays

Traditionally the RD functions have been interpreted as free decays, see e.g. Cole [1], [2], [3], [4] and extended to deal with multiple mode multiple measurements in Ibrahim [13] and [14].

The response from time t_0 to $t_0 + t$ of a structure subjected to stochastic loads consists of three parts: 1) The response from the initial displacement at the time t_0. 2) The response from the initial velocity at the time t_0. 3) The random response from the stochastic loads exciting the structure at the time t_0 to $t_0 + t$. If time segments from $X(t)$ are picked out and averaged each time $X(t) = a$ and/or $\dot{X}(t) = v$, corresponding to eqs. (6) and (8), the stochastic response will average out and the only part left will be the free decay corresponding to the initial conditions $X(t) = a$ and/or $\dot{X}(t) = v$. If the only condition is $X(t) = a$ the free decay will correspond to a step response and if the only condition is $\dot{X}(t) = v$ the free decay will correspond to an impulse response. The reason is that $X(t)$ and $\dot{X}(t)$ are independent and the mean value of $X(t)$ and $\dot{X}(t)$ is zero.

The problem if the averaging is performed at another process, $Y(t)$, see eqs. (7), (8), is whether the deterministic response can average out. Since the free decay of $X(t)$ exists and since the stochastic responses of

$X(t)$ and $Y(t)$ were recorded simultaneously on the same structure and they are dynamically coupled, it is impossible to have response from one measurement location and no response from the other.

Since RD functions are equivalent to free decays, the modal parameters can be extracted using methods as e.g. the Ibrahim Time Domain (ITD), see Ibrahim [13], [14].

4 RD and Correlation Functions

Several different papers discuss the relation between the RD functions and correlation functions. The idea was first presented in Vandiver et al. [15] and extended by Brincker et al. [16], [17] and Asmussen [12]. The assumption is that the stochastic processes are stationary Gaussian distributed with zero mean. From this assumption and the use of conditional statistics it can be proven that the RD functions calculated using $T_{X(t)}^{G_A}$ are given by

$$D_{XX}(\tau) = \frac{R_{XX}(\tau)}{\sigma_X^2} \cdot \tilde{a} - \frac{R'_{XX}(\tau)}{\sigma_X^2} \cdot \tilde{b} \qquad (15)$$

$$D_{YX}(\tau) = \frac{R_{YX}(\tau)}{\sigma_X^2} \cdot \tilde{a} - \frac{R'_{YX}(\tau)}{\sigma_X^2} \cdot \tilde{b} \qquad (16)$$

$$D_{YY}(\tau) = \frac{R_{YY}(\tau)}{\sigma_Y^2} \cdot \tilde{a} - \frac{R'_{YY}(\tau)}{\sigma_Y^2} \cdot \tilde{b} \qquad (17)$$

$$D_{XY}(\tau) = \frac{R_{XY}(\tau)}{\sigma_Y^2} \cdot \tilde{a} - \frac{R'_{XY}(\tau)}{\sigma_Y^2} \cdot \tilde{b} \qquad (18)$$

$$\tilde{a} = \frac{\int_{a_1}^{a_2} x p_X(x) dx}{\int_{a_1}^{a_2} p_X(x) dx} \qquad \tilde{b} = \frac{\int_{b_1}^{b_2} \dot{x} p_{\dot{X}}(\dot{x}) d\dot{x}}{\int_{b_1}^{b_2} p_{\dot{X}}(\dot{x}) d\dot{x}} \qquad (19)$$

and x, $\dot{x}$ are replaced by y, $\dot{y}$ if y is the triggering process. Equations (15) - (18) show how versatile the RD technique is. By adjusting the triggering levels different weights can be given to either the correlation functions or their time derivative. Furthermore, the number of triggering points is controlled by the triggering levels.

This paper will only consider the positive point triggering condition for application of the RD technique to ambient testing of linear structures. By reformulating the positive point triggering condition to

$$T_{X(t)}^{P} = \{a_1 \leq X(t) \leq a_2, -\infty < \dot{X}(t) < \infty\} \quad (20)$$

and inserting the triggering levels in eqs. (15) - (18) it is easily shown that the RD functions are proportional to the correlation functions of the processes only. The contribution from the time derivative of the correlation functions is averaged out.

5 Application to Ambient data

In application of the RD technique to identification of structures subjected to ambient excitation it is assumed that the vibrations of the structure can be modelled using a lumped mass parameter model.

$$\mathbf{M}\ddot{\mathbf{x}}(t) + \mathbf{C}\dot{\mathbf{x}}(t) + \mathbf{K}\mathbf{x}(t) = \mathbf{F}(t) \qquad (21)$$

$$\mathbf{x}(0) = \mathbf{x}_0 \qquad \dot{\mathbf{x}}(0) = \dot{\mathbf{x}}_0 \qquad (22)$$

where $\mathbf{M}$, $\mathbf{C}$ and $\mathbf{K}$ are the mass, damping and stiffness matrices of the discrete n-DOF system modelling the dynamic response at the measurement locations of the continuous structure. Using modal coordinates the free decay response is given by

$$\mathbf{x}(t) = \mathbf{\Phi} e^{\mathbf{\Lambda} t} \mathbf{q}_0 \qquad (23)$$

where $\mathbf{\Phi}$ is the mode shape matrix, $\mathbf{\Lambda}$ is a diagonal matrix with the eigenvalues of the state matrix formulated from the state equation corresponding to eq. (21) and $\mathbf{q}_0$ is the modal initial condition dependent on $\mathbf{x}_0$, $\dot{\mathbf{x}}_0$ and $\mathbf{\Phi}$. This relation is the basic equation for PTD and ITD etc. If the force vector, $\mathbf{F}(t)$ can be described as a white noise vector process passed through a linear filter, see Ibrahim et al. [19], the response are Gaussian distributed. Furthermore, the ith column of the correlation matrix of the response can be written as

$$\mathbf{R}_{\mathbf{XX}}^{i}(\tau) = \tilde{\mathbf{\Phi}} e^{\tilde{\mathbf{\Lambda}} \tau} \mathbf{c}_i \qquad (24)$$

where $\tilde{\mathbf{\Phi}}$ contains the mode shapes of the structure and the filter, $\tilde{\mathbf{\Lambda}}$ contains the eigenvalues of the structure and the filter and $\mathbf{c}_i$ is a scaling vector dependent on $\tilde{\mathbf{\Phi}}$, $\tilde{\mathbf{\Lambda}}$ and the covariance matrix of the white noise vector process, see Asmussen [12].

The results of eqs. (23) - (24) are identical except for different scaling vectors. This means that interpreting RD functions as free decays or correlation function ends up with the same final results and the same algorithm is applied to extract modal parameters. In the application of the RD technique to ambient data it is assumed that the ambient loads, wind, waves, traffic, etc., can be modelled as a filtered white vector noise process.

6 Quality Assessment

Quality assessment of RD functions has two main objectives

- Obtain information about an appropriate choice of triggering levels and RD function length prior to the full estimation of the RD matrix.
- Evaluate the accuracy of the RD functions in order to look for sets of RD functions, which should not be used in the modal parameter extraction procedures.

Before the full correlation matrix can be estimated using the RD technique the triggering levels and the RD function length have to be chosen. It is very difficult to predict an appropriate RD function length, since the chosen modal parameter estimation technique has high influence on the necessary function length. The best way is to pick out a measurement with a relatively high standard deviation. From this measurement an auto RD function is calculated using an expected high function length (e.g. ± 500 points). From a plot of this function it is easily detected when the RD function has decayed and noise becomes dominant. An example is given in section 8.

After an appropriate function length has been chosen the triggering levels should be chosen. Immediately one would choose the triggering levels which maximize the number of triggering points. But this is not always the best choice. Consider an SDOF system with $f = 1$ Hz and $\zeta = 0.01$ %. The system is loaded by white noise. To investigate the influence of the choice of triggering level 500 responses of the system are simulated. Each time series contains 5000 points and the sampling frequency is 15 Hz. For each time series the RD functions as a function of the lower and upper triggering level are calculated. By normalizing each RD function to be equal to the autocorrelation function a consistent error function can be defined as

$$\mathcal{E}_i = \frac{1}{500}\sum_{j=1}^{500}(R_{XX}(i) - \hat{R}^j_{XX}(i))^2 \qquad (25)$$

Figure 1 shows the choices of a_1, a_2 which minimize the error function. The triggering levels a_1 a_2 have been varied from 0 to $3\sigma_X$ with steps of $0.2\sigma_X$.

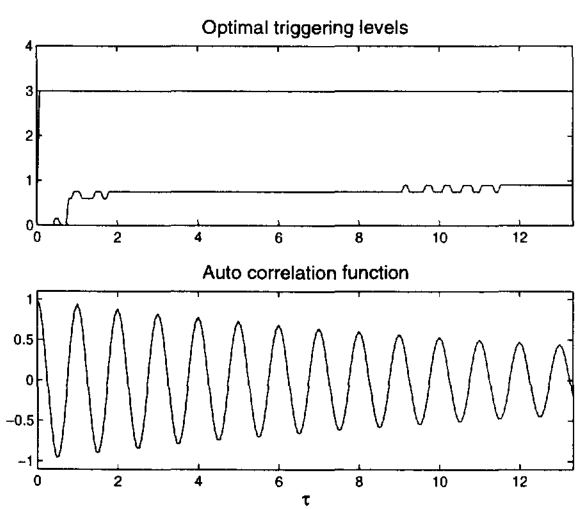

Figure 1: *Optimal choice of triggering levels for $T^P_{X(t)}$ for an SDOF system.*

As seen for this system it would be optimal to choose $[a_1\ a_2] = [\sigma_X\ \infty]$ approximately. This is a new result and very convenient since the optimal choice of triggering levels is not the triggering levels which result in the highest estimation time.

Of course the above result is only restricted to the dynamic system under consideration. So every time a new dynamic system is considered a new analysis for predicting the optimal triggering levels has to be performed. Two different methods are suggested: Shape invariance test and symmetry test.

The shape invariance test is based on several different estimations of a correlation function. It could in general be a cross correlation function, but in the preanalysis state only autocorrelation functions should be considered. The different estimates are obtained using the RD technique with different triggering levels.

$$R^1_{YX}(\tau) = \frac{D_{YX}(\tau)}{\tilde{a}_1}\sigma^2_X,\ R^2_{YX}(\tau) = \frac{D_{YX}(\tau)}{\tilde{a}_2}\sigma^2_X \ ...(26)$$

where superscripts 1, 2, ... refer to the different choices of triggering levels. In theory $R^1, R^2, ...$ should be identical due to the shape invariance of the RD functions. Two different approaches can be used to test this shape invariance. First a plot of the different correlation functions is usually sufficient to validate the different estimates. If a single estimate differs significantly from the rest, the corresponding triggering levels should not be used. If all estimates differ significantly the data should be analysed carefully by the RD technique.

If more than e.g. 5 or 6 different RD functions are estimated it might be difficult to asses the different triggering levels graphically. Instead it is suggested to calculate the correlation between the different RD functions.

$$R_{R^i_{YX}R^j_{YX}} = \frac{(\sum_{k=1}^N R^i_{YX}(k)R^j_{YX}(k))^2}{(\sum_{k=1}^N R^i_{YX}(k)^2)(\sum_{k=1}^N R^j_{YX}(k)^2)} \quad (27)$$

Theoretically the value should be unity. If different triggering levels result in a high correlation between the scaled RD functions these triggering levels are a good choice for the full estimation. The principle is illustrated in section 8.

The symmetry test is based on the symmetry relation for the correlation functions of stationary processes.

$$R_{YX}(\tau) = R_{XY}(-\tau) \qquad (28)$$

If the estimated RD functions are scaled to be equal to the correlation functions then an error function can be defined as

$$\mathcal{E}_i(\tau) = \frac{R^i_{YX}(\tau) - R^i_{XY}(-\tau)}{2} \qquad (29)$$

and a final estimate of the correlation functions can be defined as

$$R_{YX}^{i,final}(\tau) = \frac{R_{YX}(\tau) + R_{XY}(-\tau)}{2} \quad (30)$$

In order to evaluate the different RD functions estimated at different triggering levels the following error function can be used

$$\mathcal{E}_{R_{YX}^i} = \sqrt{\frac{\sum_{j=1}^{n} \mathcal{E}_i(j)^2}{\sum_{j=1}^{n} R_{YX}^{i,final}(j)}} \quad (31)$$

Equation 31 constitutes a basis for selecting the optimal choice of triggering level among a set of different triggering levels without the knowledge of the theoretically exact correlation function. In section 8 an example is given.

After the triggering levels have been selected using the above tools, the full correlation matrix can be estimated. In order to evaluate the different estimates, a time domain plot of the final estimated correlation matrix and the corresponding error function, see eqs. (29) and (30), can be performed. A better way to evaluate the correlation matrix is to plot the error defined in eq. (31) for each correlation function in the estimated correlation matrix. This makes it possible to detect erroneous sets of correlation functions in a simple manner. The principle is illustrated in section 8.

The final step in quality assessment of RD functions is to average the absolute value of the Fourier transform of all estimated correlation functions. This is a simple way to compress the information from all correlation functions in a single plot. Usually it is very simple to detect the modes of the structure from this plot and use it as information prior to the modal parameters extraction procedure.

7 Modal Parameters

The modal parameters can be extracted from the estimated correlation matrix using methods like Polyreference Time Domain (PTD), see Vold et al. [20] or Ibrahim Time Domain, see Ibrahim [21], which were developed to extract modal parameters from free decays.

From the quality assessment procedures the number of modes and the approximate natural frequencies of the modes are known. This is valuable information when the number of modes has to be selected for the input to the above algorithms. The main task is to separate the noise modes from the physical modes. To do this, modal confidence factors, see Ibrahim [22] or Vold et al. [23], modal participation factors, the demand of complex conjugate modes and low damping ratios are applied.

8 Example - Concrete Bridge

To illustrate the given guidelines for identification of structures subjected to ambient loads an ambient test of the Vestvej bridge is considered. The Vestvej bridge is a two-span concrete bridge over the highway between Aalborg and Frederikshavn just north of Aalborg, Denmark. The ambient testing of the Vestvej was performed on August 22, 1997. The bridge was loaded mainly by the vehicles passing the bridge, but also wind and trucks passing under the bridge contributed to the dynamic response of the bridge.

Figure 2: *The Vestvej bridge.*

The illustration is delimited to identification of the right-hand span only. An outline draft of the Vestvej bridge and the measurement locations is shown in fig. 3.

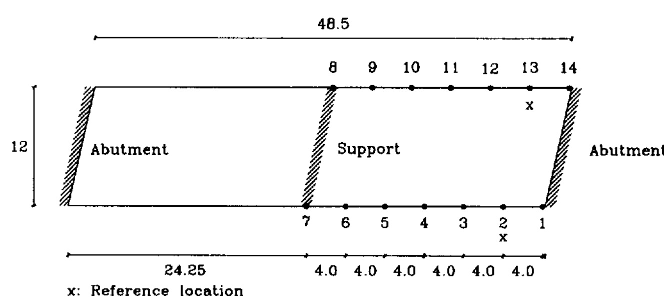

Figure 3: *Outline draft of the Vestvej bridge and the measurement locations. Distances in* m.

The accelerations of the bridge were recorded using Schaewitz accelerometers with a sensitivity of ± 0.25 g. The accelerations were recorded for 900 seconds at 320 Hz. No analog filter was applied, since none of the ambient loads are exciting the structure above 160 Hz. In order to reduce the noise content the data were filtered digitally and decimated to end up with a resulting sampling frequency of 80 Hz and 72000 points in each measurement. Two reference locations are selected: 2 and 13. The responses of the bridge have been collected in two measurement setups with simultaneously recorded measurements. The measurements in each setup are shown in table 1 together with the standard deviation of the measurements.

Meas. No.	Setup 1	σ_X [g]	Setup 2	σ_X [g]
1	2	0.0060	2	0.0071
2	13	0.0063	13	0.0072
3	1	0.0018	3	0.0103
4	14	0.0017	2	0.0109
5	6	0.0088	4	0.0113
6	7	0.0035	5	0.0072
7	9	0.0057	11	0.0079
8	8	0.0065	10	0.0107

Table 1: *Setup number and measurement location.*

A time domain plot of measurement 5 in setup 2 is shown in fig. 4.

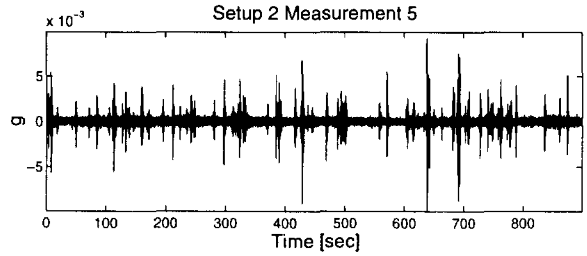

Figure 4: *Time domain plot of data from measurement location 4.*

In order to find the necessary number of points in the RD functions the measurement shown in fig. 4 is considered, since it has the highest standard deviation. The auto RD function is calculated using positive point triggering with $[a_1\ a_2] = [\sigma_X \infty]$ and ± 500 points corresponding to ± 6.25 s.

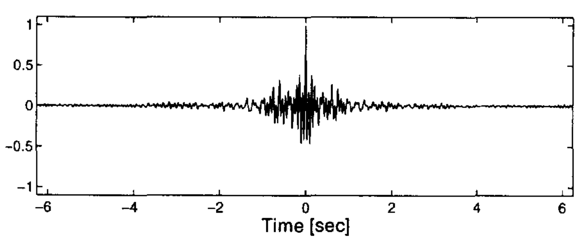

Figure 5: *Initial auto RD function of measurement 5 setup 2, N=4340.*

From fig. 5 it is seen that ± 500 points are too many. Instead ± 250 is chosen. In order to determine the optimum triggering levels the auto RD functions are calculated from each measurement with different choice of triggering levels, $[a_1\ a_2] = [a_1^i \sigma_X\ \infty]$, $a_1^i = 0, 0.5, 1.0, 1.5, 2.0, 2.5, 3.0$. For each of these RD functions (normalized) the error function and the final estimate are calculated using eqs. (29) and (30) and the error measure in eq. (31) are calculated. Figures 6 and 7 show the errors for each measurement as a function of the lower triggering level.

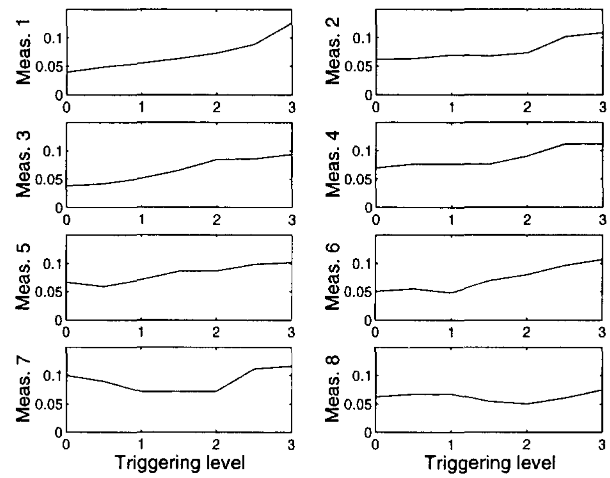

Figure 6: *Error measures for the auto RD functions for setup 1 as a function of the lower triggering level.*

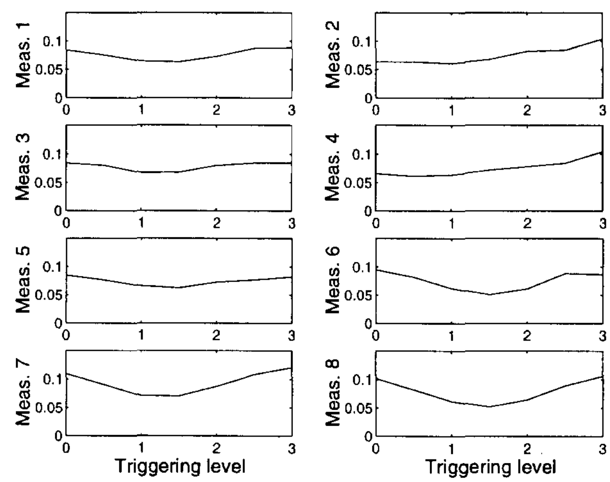

Figure 7: *Error measures for the auto RD functions for setup 2 as a function of the lower triggering level.*

The errors show that it would not be optimal to choose $[a_1\ a_2] = [0\ \infty]$, which would result in the highest number of averages. Instead it is chosen to use $[a_1\ a_2] = [\sigma_X\ \infty]$.

The correlation between each estimated RD function is calculated for measurement 5 setup 2 and plotted in fig. 8 as a function of the lower triggering level.

It is seen that there is a high correlation between the RD functions from $a_1^i = 1, 1.5, 2, 2.5, 3$, wheras the correlation between the RD function from $a_1^i = 0, 0.5$ and $a_1^i = 1, 1.5, 2, 2.5, 3$ is low. This supports the choice of $[a_1\ a_2] = [\sigma_x\ \infty]$.

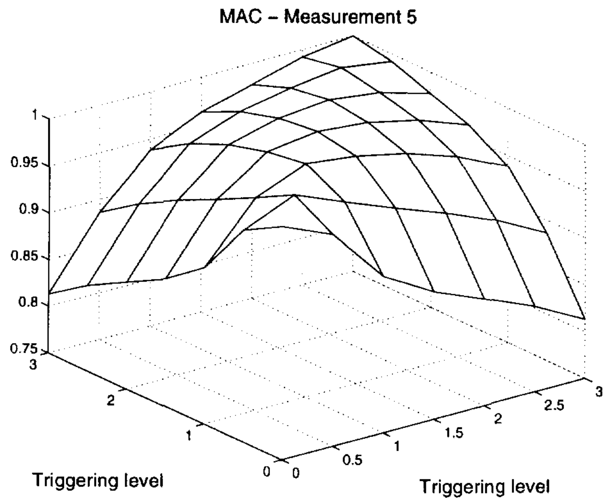

Figure 8: *Correlation between RD functions for measurement 5 setup 2.*

All cross and auto RD functions are calculated with ± 250 points and $[a_1\ a_2] = [\sigma_X\ \infty]$. Before the modal parameters are extracted an average spectral density is calculated from the sum of the Fourier transform of each of the RD functions. The result is shown in fig. 9. It seems that 9 different modes with the frequencies [5.08 6.64 7.97 8.20 8.83 13.05 13.28 14.53 14.77] Hz are present in the measurements.

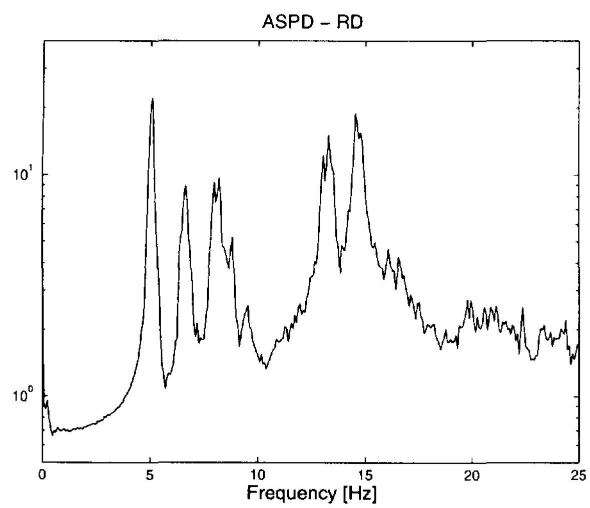

Figure 9: *Average spectral densities of the measurements calculated using the RD algorithm.*

In order to evaluate the estimated RD functions the error for each RD function is calculated and plotted in fig. 10.

As seen the error for each function has approximately the same level. None of the sets of RD functions has significantly higher error than the others. This means that all estimated sets of RD functions can be used in the modal parameter extraction process. The analysis of setup 2 gave an equal result.

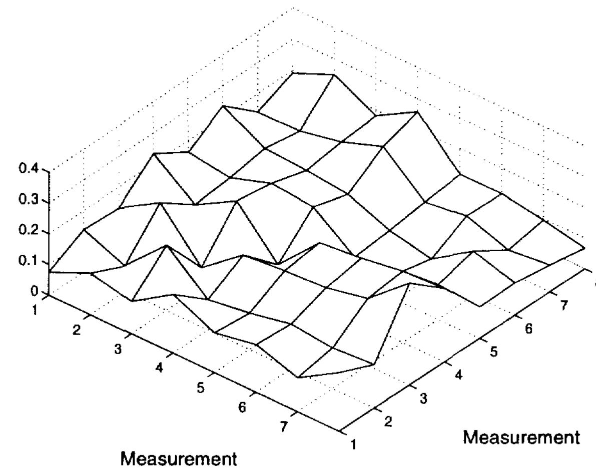

Figure 10: *The error of the RD matrix for setup 1 calculated using eq. (31).*

The modal parameters are extracted from the RD matrices using PTD. The number of modes was varied from 20 to 30 and the number of points used from the final RD matrices was varied from 100 to 120. Stabilization diagrams together with a demand of low damping ratios and high modal confidence factors were used to extract physical modes. Table 2 shows the modes which resulted in mode shapes with high confidence.

f [Hz]	5.05	6.59	7.99	9.71	13.24	14.68
ζ [%]	2.82	3.74	3.52	2.09	1.72	2.33

Table 2: *Estimated frequencies and damping ratios.*

The mode shape corresponding to the three first modes are shown in fig. 11.

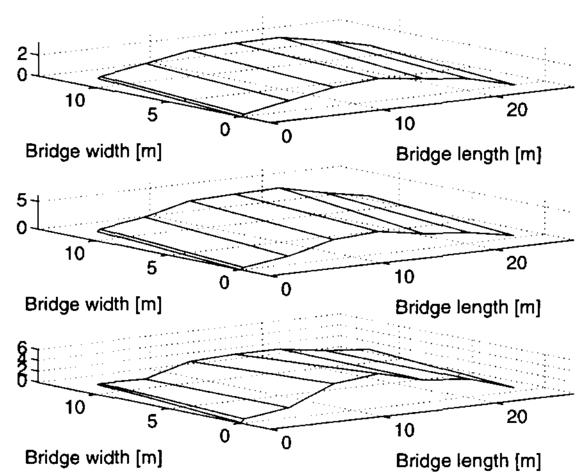

Figure 11: *Mode shape for the first 3 modes of the bridge.*

9 Conclusion

The theory behind the Random Decrement technique has been discussed together with the implementation of the technique. Different formulations of the triggering levels are shown and it is recommended to use the positive point triggering condition to analyse ambient data.

A new concept: Quality Assessment has been introduced. The purpose is to give a method to select the triggering levels prior to the estimate of Random Decrement functions and to perform an evaluation of the estimates of RD functions.

The technique has been illustrated by an analysis of the ambient response of a concrete bridge.

10 Acknowledgement

Financial support from the Danish Technical Research Council is gratefully acknowledged.

References

[1] Cole, H.A. *On-The-Line Analysis of Random Vibrations.* AIAA Paper No. 68-288. 1968.

[2] Cole, H.A. *Method and Apparatus for Measuring the Damping Characteristics of a Structure.* United States Patent No. 3, 620,069, Nov. 16. 1971.

[3] Cole, H.A. *Failure Detection of a Space Shuttle Wing by Random Decrement.* NASA TMX-62,041, May 1971.

[4] Cole, H.A. *On-Line Failure Detection and Damping Measurements of Aerospace Structures By Random Decrement Signature.* NASA CR-2205, 1973.

[5] Nasir, J. & Sunder, S.S. *Evaluation of the Random Decrement Technique of Vibration Signature Analysis for Monitoring of Offshore Platforms.* Massachusetts Institute of Technology, Department of Civil Engineering, Research Report R82-52. Sept. 1982.

[6] Siviter, R. & Pollard, M.G. *Measurement of Railway Vehicle Kinematic Behaviour Using the Random Decrement Technique.* The Shock and Vibration Bulletin, Bulletetin 55, Part 3 of 5, June 1985, pp. 57-66.

[7] Al-Sannad, H.A., Aggour, M.S. & Amer, M.I. *Use of Random Loading in Soil Testing.* Indian Geotechnical Journal, Vol. 16, No. 2, April 1986, pp. 126-135.

[8] Asmussen, J.C., Ibrahim, S.R. & Brincker, R. *Random Decrement and Regression Analysis of Traffic Responses of Bridges.* Proc. 14th International Modal Analysis Conference, Dearborn, Michigan, USA, February 1996, Vol I, pp. 453-458.

[9] Asmussen, J.C., Ibrahim, S.R. & Brincker, R. *Application of Vector Triggering Random Decrement.* Proc. 15th International Modal Analysis Conference, Orlando, Florida, USA, February 3-6 1997, Vol II, pp. 1165-1171.

[10] Asmussen, J.C., Brincker, R., Rytter, A. & Hededal, P. *Ambient Testing of the Vestvej Bridge Using Random Decrement.* To be presented at the 16th International Modal Analysis Conference, Santa Barbara, California, USA, February 1998.

[11] Fasana, A., Garibaldi, L., Giorcelli, E, Ruzzene, M. & Sabia, D. *Analysis of a Motorway Bridge Under Random Traffic Excitation.* Proc. 15th International Modal Analysis Conference, Orlando, Florida, USA, February 3-6 1997, Vol I, pp. 293-300.

[12] Asmussen, J.C. *Modal Analysis Based on the Random Decrement Technique - Applications to Civil Enginering Structures.* Ph.D.-thesis Aalborg University, Denmark, August 1997.

[13] Ibrahim, S.R. *Random Decrement Technique for Modal Identification of Structures.* Journal of Spacecraft and Rockets, Vol. 14, No. 11., Nov. 1977, pp. 696-700.

[14] Ibrahim, S.R. *The Use of Random Decrement Technique for Identification of Structural Modes of Vibration.* AIAA paper, Vol. 77, 1977, pp. 1-9.

[15] Vandiver, J.K., Dunwoody, A.B., Campbell, R.B. & Cook, M.F. *A Mathematical Basis for the Random Decrement Vibration Signature Analysis Technique.* Journal of Mechanical Design, Vol. 104, April 1982, pp. 307-313.

[16] Brincker, Krenk, S. & R., Jensen, J.L. *Estimation of Correlation Functions by the Random Dec Technique.* Proc. Skandinavisk Forum for Stokastisk Mekanik, Lund, Sweden, Aug. 30-31, 1990.

[17] Brincker, R., Krenk, S. & Jensen, J.L. *Estimation of Correlation Functions by the Random Decrement Technique.* Proc. 9th International Modal Analysis Conference and Exhibit, Firenze, Italy, April 14-18, 1991.

[18] Brincker, R., Krenk, S., Kirkegaard, P.H. & Rytter, A. *Identification of Dynamical Properties from Correlation Function Estimates.* Bygningsstatiske Meddelelser, Vol. 63, No. 1, 1992, pp. 1-38.

[19] Ibrahim, S.R., Asmussen, J.C. & Brincker, R. *Modal Parameter Identification from Responses of General Unkonwn Random Inputs.* Proc. 14th International Modal Analysis Conference, Dearborn, Michigan, USA, February 1996, Vol I, pp. 446-452.

[20] Vold, H., Kundrat, J., Rocklin, G.T. & Russel, R. *A Multi-Input Modal Estimation Algorithm for Minicomputers.* SAE Paper No. 820194, 1982

[21] Ibrahim, S.R. *An Upper Hessenberg Sparse Matrix Algorithm for Modal Identification on Minicomputers.* Journal of Sound and Vibration, (1987) 113(1) pp. 47-57.

[22] Ibrahim, S.R. *Modal Confidence Factor in Vibration Testing.* Journal of Spacecraft, Sept.-Oct. 1978 Vol. 15, No. 5, pp. 313-316.

[23] Vold, H. & Crowley, J. *A Modal Confidence Factor for the Polyreference Time Domain Technique.* Proc. 3rd International Modal Analysis Conference, 1985, pp. 305-310.